Available online at www.sciencedirect.com
SCIENCE DIRECT®
Neuropharmacology 47 (2004) 17–34
NEURO PHARMACOLOGY
www.elsevier.com/locate/neuropharm

Abolition of zolpidem sensitivity in mice with a point mutation in the $GABA_A$ receptor $\gamma 2$ subunit

D.W. Cope [a,*], P. Wulff [b], A. Oberto [c,1], M.I. Aller [b], M. Capogna [a], F. Ferraguti [a,2], C. Halbsguth [a], H. Hoeger [d], H.E. Jolin [c], A. Jones [c,3], A.N.J. Mckenzie [c], W. Ogris [e], A. Poeltl [e], S.T. Sinkkonen [f], O.Y. Vekovischeva [f], E.R. Korpi [f,g], W. Sieghart [e], E. Sigel [h], P. Somogyi [a], W. Wisden [c,4]

[a] *MRC Anatomical Neuropharmacology Unit, Department of Pharmacology, Oxford University, Mansfield Road, Oxford OX1 3TH, UK*
[b] *Department of Clinical Neurobiology, University of Heidelberg, Im Neuenheimer Feld 364, D-69120 Heidelberg, Germany*
[c] *MRC Laboratory of Molecular Biology, Hills Road, Cambridge CB2 2QH, UK*
[d] *Department of Laboratory Animal Science and Genetics, Medical University Vienna, Brauhausgasse 34, 2325 Himberg, Austria*
[e] *Brain Research Institute, Division of Biochemistry and Molecular Biology, Medical University Vienna, Spitalgasse 4, A-1090 Vienna, Austria*
[f] *Institute of Biomedicine, Pharmacology, Biomedicum Helsinki, University of Helsinki, FIN-00014 Helsinki, Finland*
[g] *Department of Pharmacology and Clinical Pharmacology, University of Turku, FIN-20520 Turku, Finland*
[h] *Department of Pharmacology, University of Bern, Friedbuhlstrasse 49, CH-3010 Bern, Switzerland*

Received 3 December 2003; received in revised form 3 February 2004; accepted 1 March 2004

Abstract

Agonists of the allosteric benzodiazepine site of $GABA_A$ receptors bind at the interface of the α and γ subunits. Here, we tested the in vivo contribution of the $\gamma 2$ subunit to the actions of zolpidem, an $\alpha 1$ subunit selective benzodiazepine agonist, by generating mice with a phenylalanine (F) to isoleucine (I) substitution at position 77 in the $\gamma 2$ subunit. The $\gamma 2$F77I mutation has no major effect on the expression of $GABA_A$ receptor subunits in the cerebellum. The potency of zolpidem, but not that of flurazepam, for the inhibition of [^{3}H]flunitrazepam binding to cerebellar membranes is greatly reduced in $\gamma 2$I77/I77 mice. Zolpidem (1 μM) increased both the amplitude and decay of miniature inhibitory postsynaptic currents (mIPSCs) in Purkinje cells of control C57BL/6 (34% and 92%, respectively) and $\gamma 2$F77/F77 (20% and 84%) mice, but not in those of $\gamma 2$F77I mice. Zolpidem tartrate had no effect on exploratory activity (staircase test) or motor performance (rotarod test) in $\gamma 2$I77/I77 mice at doses up to 30 mg/kg (i.p.) that strongly sedated or impaired the control mice. Flurazepam was equally effective in enhancing mIPSCs and disrupting performance in the rotarod test in control and $\gamma 2$I77/I77 mice. These results show that the effect of zolpidem, but not flurazepam, is selectively eliminated in the brain by the $\gamma 2$F77I point mutation.
© 2004 Elsevier Ltd. All rights reserved.

Keywords: $GABA_A$ receptor; $\gamma 2$ subunit; mIPSC; Zolpidem; Benzodiazepine; Cerebellum

1. Introduction

Ligands for the $GABA_A$ receptor allosteric benzodiazepine (BZ) binding site modulate current flow through the receptor by altering the efficacy of GABA for opening the anion channel (Sieghart, 1995; Korpi et al., 2002). Zolpidem, an imidazopyridine BZ site ligand, is a widely used hypnotic. It has some selectivity for receptors containing the $\alpha 1$ subunit, which is present in a major $GABA_A$ receptor population in the rodent brain (Puia et al., 1991; Sieghart, 1995; Sur et al., 2001; Kralic et al., 2002; Sieghart and Sperk, 2002). In vitro, zolpidem potentiates action potential-

* Corresponding author. Present address: School of Biosciences, Cardiff University, Museum Avenue, Cardiff CF10 3US, UK. Tel.: +44-2920-879113; fax: +44-2920-874986.
E-mail address: copedw@cf.ac.uk (D.W. Cope).
[1] Present address: Department of Pharmacology, and Department of Anatomical, Pharmacological and Forensic Medicine, Via Pietro Giuria, 13, University of Turin, Turin 10125, Italy.
[2] Present address: Department of Pharmacology, University of Innsbruck, Peter-Mayr-Strasse 1a, A-6020 Innsbruck, Austria.
[3] Present address: Department of Optometry, Anglia Polytechnic University, East Road, Cambridge CB1 1PT, UK.
[4] Present address: Department of Clinical Neurobiology, University of Heidelberg, Im Neuenheimer Feld 364, D-69120 Heidelberg, Germany.

0028-3908/$ - see front matter © 2004 Elsevier Ltd. All rights reserved.
doi:10.1016/j.neuropharm.2004.03.007

evoked (spontaneous) and quantal (miniature) GABAergic synaptic transmission by increasing the decay and sometimes the amplitude of synaptic currents (e.g. De Koninck and Mody, 1994; Perrais and Ropert, 1999; Hájos et al., 2000). Furthermore, action potential-evoked postsynaptic potentials are potentiated by zolpidem in a multiphasic time-dependent manner often to a greater extent than expected from the potentiation of miniature synaptic currents (Thomson et al., 2000). Mice containing a point mutation in the α1 subunit gene (α1H101R) that abolishes the binding of BZs and zolpidem have been used to clarify which behavioural effects of zolpidem are mediated by α1 subunit-containing $GABA_A$ receptors (Rudolph et al., 1999; Crestani et al., 2000; McKernan et al., 2000). Synaptic currents evoked by GABA in these mice have reduced zolpidem sensitivity (Bacci et al., 2003).

The BZ binding site occurs at the interface of the α and γ subunits (Sigel, 2002; Ernst et al., 2003). Point mutation studies on recombinant receptors revealed residues within the BZ binding pocket of the γ2 subunit necessary for zolpidem binding (Buhr et al., 1997; Wingrove et al., 1997). The substitution of phenylalanine (F) to isoleucine (I) at position 77 in the mature γ2 subunit reduced zolpidem binding without altering the binding of BZ agonists such as diazepam and flunitrazepam (Buhr et al., 1997; Wingrove et al., 1997). This selective effect provided an opportunity to test the basis of the γ2 subunit-mediated action of zolpidem in vivo by generating mice that carry the γ2F77I point mutation. Such a mutation at a drug binding site is unlikely to affect the binding and effect of synaptically released GABA and might be considered as equivalent to "a neutral gene polymorphism", which nevertheless may influence nervous system function. Indeed, strain background has marked influences on how BZs affect mice in behavioural tasks (e.g. Belzung et al., 2000; Griebel et al., 2000). In addition to behavioural tests, we have compared miniature inhibitory postsynaptic currents (mIPSCs) from cerebellar Purkinje and stellate/basket cells because these cell types express the α1 and γ2 subunits (Wisden et al., 1992; Pirker et al., 2000; reviewed in Wisden et al., 1996). Some of these data have been previously reported as an abstract (Cope et al., 2003).

2. Materials and methods

2.1. Generation of the $GABA_A$ receptor subunit γ2F77I point mutant mice

The F77 position of the mature γ2 $GABA_A$ receptor subunit is encoded within exon 4 of the cognate gene. A targeting vector was designed such that after homologous recombination in mouse embryonic stem cells, the F77 codon was replaced with one encoding I77 (Fig. 1A). The genomic region containing the $GABA_A$ receptor γ2 subunit (gabrg2, gene reference number ENSMUSG00000020436; www.ensembl.org/Mus_musculus/geneview) was obtained on a bacterial artificial chromosome (BAC) by screening a mouse 129 BAC library (BAC Mouse ES release I, BAC 4921, Genome Systems Inc, USA). An approximately 6 Kb HindIII

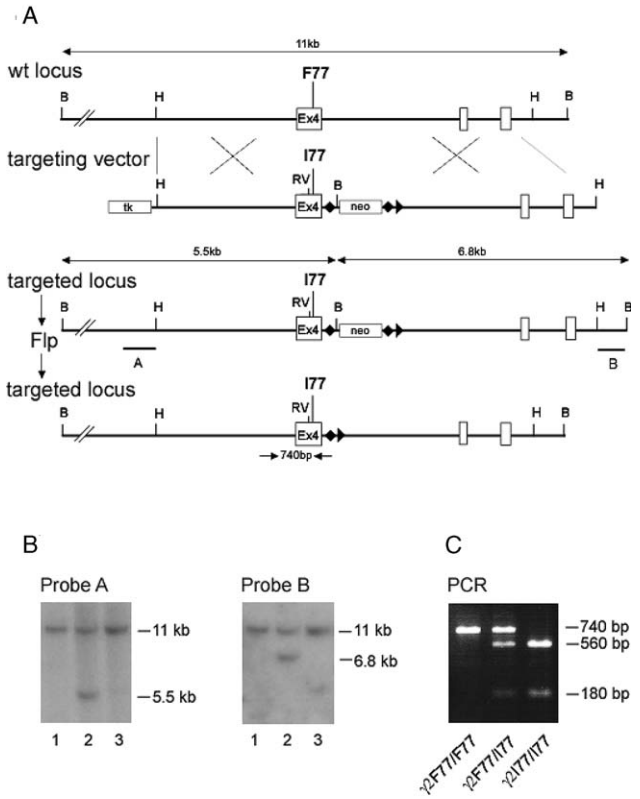

Fig. 1. Generation of $GABA_A$ receptor γ2F77I mutant mice. (A) Targeting strategy. A mutation changing the codon of phenylalanine (F) to isoleucine (I) at position 77 was inserted along with an EcoRV (RV) site into the fourth exon (Ex4) of the γ2 subunit gene. For the initial targeting the neomycin resistance cassette (neo) was flanked by two frt sites (black diamonds) and cloned into intron four; the neomycin resistance cassette contains a single loxP site (black triangle) at the 3′ end. The targeting vector contained an HSV thymidine kinase (tk) at the 5′ end for negative selection. After gene targeting the neo was removed by transient transfection with Flp-recombinase. Open boxes indicate exons. B indicates BglII restriction sites, H, indicates HindIII restriction sites, black bars labelled A and B indicate the 5′ and 3′ external probes used for Southern blot analysis. Expected fragment sizes of the wild-type and targeted γ2 locus are also indicated. Arrows below the targeted locus indicate PCR primers used for genotyping. The number between the arrows indicates the size of the amplified fragment; (B) Southern blots of BglII-digested ES cell DNA after gene targeting hybridised with probe A and B, respectively. Lane 2 shows a targeted ES cell clone, lanes 1 and 3 non-targeted ES cell clones. (C) Genotyping of mouse tail DNA by PCR and EcoRV digest. The amplified fragment of wild-type γ2F77/F77 mice is not cut by EcoRV and gives a 740 bp band. In heterozygous F77/I77 and point mutant γ2I77/I77 mice the fragment is cut by EcoRV and gives rise to a 560 and a 180 bp bands.

fragment, containing exon 4 of the γ2 subunit gene, was subcloned from the BAC into pBluescript (Stratagene) to provide the targeting vector backbone (Fig. 1A). The native γ2 subunit peptide sequence determining zolpidem sensitivity is EYTIDIFFAQTWY (Buhr et al., 1997; Wingrove et al., 1997); the underlined residue is the crucial amino acid. Using a Stratagene QuickChange Site-Directed mutagenesis kit, we changed exon 4 in the targeting vector to encode EYTIDIIFAQTWY, and at the same time introduced an EcoRV site to help identify the mutant allele (Fig. 1A). The oligonucleotides used were: F77IS, 5′-CAG GAA TAT ACA ATT GAT AT***C A***TT TTT GCC CAA ACC TGG TAT G-3′; and F77IAS, 5′-CAT ACC AGG TTT GGG CAA AAA ***TG***A TAT CAA TTG TAT ATT CCT G-3′. The two changed nucleotides from wild-type are underlined. Similarly, we mutated an AflII site in intron 4 into an XhoI site (primers 5′-GGG ATA GAA AAG GAT TCT CGA GAC TCT TTG CCT TCT ATC TTG-3′; and 5′-CAA GAT AGA AGG CAA AGA GTC TCG AGA ATC CTT TTC TAT CCC-3′) and then inserted an "frt-HSV-neomycin resistance gene-frt-loxP" cassette (Oberto, Mckenzie and Wisden, unpublished) into this new XhoI site. An internal BglII site within this cassette creates the polymorphism used to detect homologous recombination events (Fig. 1A). The loxP site has no functional relevance for any procedures described here; it is simply an integral part of the particular neo cassette we used, and so was carried into the targeting vector construct with the subcloning of the cassette. Finally, an HSV-thymidine kinase gene, driven by an HSV promoter for negative selection (Jones et al., 1997), was placed into the targeting vector's polylinker. Before transfection into the embryonic stem cell line E14.1 (129ola, a gift from K. Rajewsky, Köln, Germany), the targeting vector was linearised with NotI. We identified two correctly targeted colonies (γ2F77I-neo) out of 288 screened by Southern blotting; colony genomic DNA was digested with BglII and hybridised consecutively with flanking probes A and B (Fig. 1B).

We next removed, by Flp-mediated recombination, the neomycin resistance gene from intron 4, leaving only a loxP-frt "scar" (Fig. 1A). For this, the γ2F77I-neo ES cell colonies were expanded and transfected with an Flp recombinase expression vector, pCAGGS-Flpe (Schaft et al., 2001). Colonies that were negative for neomycin resistance gene insertions, as analysed by Southern blotting, were then regenotyped and confirmed for the F77I mutation, and by sequencing of a PCR product amplified from a region across exon 4. A correctly targeted γ2F77I stem cell clone with the neo gene removed was injected into blastocysts and male chimeras mated with wild-type C57BL/6J (i.e. C57BL/6J × 129ola) to produce the F1 generation of the γ2F77I line. We amplified by PCR the entire exon 4 region from genomic DNA of the F1 γ2F77/I77 mice and sequenced it to confirm the mutation (data not shown); the γ2F77I subunit gene in the final line differs from the wild-type in having two nucleotides changed in exon 4, and the loxP-frt scar in intron 4. The line is genotyped routinely by PCR on genomic DNA using primers (5′-TCA TAA CTT CTA GTA TGT TGT CTT-3′ (sense, intron 3); and 5′-ACC ATC ATT CCA AAT TCT CAG CAT-3′ (antisense, exon 4)) that amplify a region across exon 4 followed by digestion of the product with EcoRV (Fig. 1C). The wild-type γ2F77 allele gives a 740 bp band, whereas the γ2I77 allele gives 560 and 180 bp bands. Heterozygous γ2F77/I77 breeding pairs were crossed to give homozygous point mutant and wild-type littermate controls for the experiments. Mice from different generations were used. No attempt was made to make the line congenic, therefore C57BL/6J mice were included throughout the electrophysiological and behavioural experiments as a control.

2.2. Quantitative immunoblot analysis of $GABA_A$ receptor subunits

A total of six γ2F77/F77 and five γ2I77/I77 adult mouse cerebella were individually homogenised using an Ultra-Turrax® in 50 mM Tris/citrate buffer (pH 7.1), containing one complete protease inhibitor cocktail tablet per 50 ml buffer (Roche Diagnostics, Mannheim, Germany). The suspensions were pressed through a set of needles with increasingly small diameters using a syringe. Equal amounts (containing 7 μg of protein) of the suspension were subjected to sodium dodecyl sulphate-polyacrylamide gel electrophoresis (SDS-PAGE) in different slots of the same 10% polyacrylamide gel. Proteins were blotted to polyvinylidene difluoride membranes and detected by antibodies to the following subunits: α1 (amino acid residues 1–9); α6 (317–371); β2 (351–405); β3 (345–408); γ2 (319–366); and δ (1–44) (Jechlinger et al., 1998; Pöltl et al., 2003). Secondary antibodies ($F_{(ab')2}$ fragments of goat anti-rabbit IgG, coupled to alkaline phosphatase; $F_{(ab')2}$ fragments of goat anti-mouse IgG, coupled to alkaline phosphatase, Axell, Westbury, NY, USA) were visualised by the reaction of alkaline phosphatase with CDP-Star (Applied Biosystems, Bedford, MA, USA). The chemiluminescent signal was quantified by densitometry after exposing the immunoblots to the Fluor-S MultImager (Bio-Rad Laboratories, Hercules, CA) and evaluated using Quantity One Quantitation Software (Bio-Rad Laboratories) and GraphPad Prism (GraphPad Software Inc., San Diego, CA). Quantification was performed by an independent investigator blind to the identity of the samples. The linear range of the detection system was established by measuring the antibody

signal generated to a range of antigen concentrations. Under the experimental conditions used, the immunoreactivities were within the linear range, and this permitted a direct comparison of the amount of antigen per gel lane between samples. The amounts of individual $GABA_A$ receptor subunits present in homogenates from γ2I77/I77 and γ2F77/F77 mice were compared in the same gel. Data were generated from two to four different gels per subunit and per mouse, and are expressed as mean ± standard deviation. Student's unpaired *t*-test was used for comparing groups, and significance was set at $P < 0.05$.

2.3. Preparation of receptor extracts and immunoprecipitation for receptor binding studies

Cerebella from a total of nine γ2F77/F77 and eight γ2I77/I77 adult mice were homogenised individually in 50 mM Tris/citrate buffer (pH 7.1) containing one complete protease inhibitor cocktail tablet per 50 ml buffer as described above. After the removal of aliquots for protein determination and western blot analysis, homogenates of three cerebella were pooled and centrifuged at $100,000\times g$. The centrifugation pellet was then suspended in 5 ml of a deoxycholate buffer (0.5% deoxycholate, 0.05%, phosphatidylcholine, 10 mM Tris–HCl, 150 mM NaCl, 1 complete protease inhibitor cocktail tablet per 50 ml, pH 8.5) followed by incubation under intensive stirring for 1 h at 4 °C. After centrifugation at $150,000\times g$ for 45 min the clear supernatant was used for subsequent immunoprecipitation and GABA-sensitive [^{3}H]muscimol binding studies. For the determination of the solubilisation efficiency of individual $GABA_A$ receptor subunits as well as of functional receptors, the $150,000\times g$ pellet was re-dissolved in the same volume of deoxycholate buffer. Aliquots of this suspension as well as aliquots from the clear supernatant of the $150,000\times g$ centrifugation were separately subjected to protein precipitation using the methanol/chloroform method (Wessel and Flügge, 1984), followed by SDS-PAGE and quantitative western blot analysis.

For immunoprecipitation, 50 or 100 μg protein of the clear supernatant as well as of the re-dissolved $150,000\times g$ pellet were mixed with a solution containing 5 μg of α1 (1–9), 10 μg of β1 (350–404), 5 μg of β2 (351–405), and 5 μg of β3 (345–408) antibody in order to precipitate all $GABA_A$ receptors present in the cerebellar extract. This antibody composition was used because all functional $GABA_A$ receptors are supposed to contain at least one of the three β subunits, and most of them contain an α1 subunit (Jechlinger et al., 1998; Pöltl et al., 2003). The mixture was then incubated under gentle shaking at 4 °C overnight. Then 50 μl of pansorbin (Calbiochem, La Jolla, CA, USA) and 50 μl 5% dry milk powder, both in low salt buffer for immunoprecipitation (IP-low; 50 mM Tris–HCl, 150 mM NaCl, 1 mM EDTA, 0.2% Triton X-100, pH 8.0), were added and incubation was continued for 2 h at 4 °C under gentle shaking. The precipitate was centrifuged for 6 min at $2,300\times g$, washed twice with 500 μl of high salt buffer for immunoprecipitation (IP-high; 50 mM Tris–HCl, 600 mM NaCl, 1 mM EDTA, 0.5% Triton X-100, pH 8.3) and once with 500 μl of IP-low. The precipitated receptors were suspended in 1 ml of solution containing 0.1% Triton X-100, 50 mM Tris/citrate buffer and 1–40 nM [^{3}H]muscimol (29.5 Ci/mmol, PerkinElmer Life Sciences) in the absence or presence of 1 mM GABA. After incubation for 1h at 4 °C the suspensions were rapidly filtered through Whatman GF/B filters, washed twice with 3.5 ml of 50 mM Tris/citrate buffer and subjected to liquid scintillation counting (Filter-Count™, Packard; 2100 TR Tri-Carb® Scintillation Analyser, Packard). Binding in the presence of 1 mM GABA (unspecific binding) was then subtracted from binding in the absence of GABA (total binding), resulting in specific binding to precipitated $GABA_A$ receptors. Data were analysed using GraphPad Prism.

2.4. Inhibition of [^{3}H]flunitrazepam binding

Cerebella from a total of three γ2F77/F77 and three γ2I77/I77 adult mice were homogenised individually in 50 mM Tris/citrate buffer (pH 7.1), as described above. The homogenates were ultracentrifuged at $150,000\times g$, the pellets washed three times and finally resuspended in 12 ml of a 50 mM Tris/citrate buffer (pH 7.1). For inhibition studies, 300 μl of the suspension was added to a final volume of 1 ml of a solution containing: 50 mM Tris/citrate buffer (pH 7.1); 150 mM NaCl; 5 nM [^{3}H]flunitrazepam (71.0 Ci/mmol, PerkinElmer Life Sciences). In addition, one of the following drugs was included: zolpidem (1 nM–1 mM), flumazenil (300 pM–1 μM) or flurazepam (1 nM–10 μM), in the absence or presence of 100 μM flunitrazepam. After incubation for 90 min at 4 °C, the suspensions were rapidly filtered through Whatman GF/B filters, washed twice with 5 ml of 50 mM Tris/citrate buffer (pH 7.1) and subjected to liquid scintillation counting. Data were analysed using GraphPad Prism.

For determining possible alterations in [^{3}H]flunitrazepam binding Scatchard analysis was performed. For each experiment, homogenates of two γ2F77/F77 and two γ2I77/I77 cerebella were prepared, ultracentrifugated and washed as described above, and 100 μl of the final homogenates was added to a final volume of 1 ml of a solution containing: 50 mM Tris/citrate buffer (pH 7.1); 150 mM NaCl; and 1–50 nM [^{3}H]flunitrazepam (84.5 Ci/mol, PerkinElmer Life Sciences) in the absence or presence of 10 μM unlabelled flunitrazepam. After incubation

for 90 min at 4 °C the suspensions were rapidly filtered, washed, subjected to liquid scintillation counting and analysed, as described above.

2.5. Immunocytochemistry of $GABA_A$ receptors

Three adult γ2I77/I77 and three adult γ2F77/F77 mice (25–30 g) were deeply anaesthetised with sodium pentobarbital (100 mg/kg, i.p.) and transcardially perfused in accordance with the UK Animals (Scientific Procedure) Act 1986. The first solution was 0.1 M phosphate-buffered (PB) 0.9% saline, followed by a fixative composed of 4% paraformaldehyde and ~0.2% picric acid made up in 0.1 M PB (pH 7.2) for 7 min. Brains were quickly removed, extensively rinsed in PB and 50 μm thick sagittal sections cut on a vibratome. Immunocytochemical reactions were performed according to the indirect avidin–biotin–HRP complex procedure (Vectastain ABC Elite kit, Vector Laboratories, Burlingame, CA, USA) as described previously (Somogyi et al., 1989), with minor modifications. Free-floating sections were pre-incubated (1 h) with 20% normal goat serum (NGS) in Tris-buffer saline (TBS), and subsequently incubated with primary antibodies (72 h, 4 °C) in a solution composed of 1% NGS and 0.3% Triton-X 100 in TBS. Affinity purified primary antibodies to the α1 (0.6 μg/ml), β3 (1 μg/ml) and γ2 (1 μg/ml) subunits were the same as used for immunoblotting. In addition affinity purified guinea pig polyclonal anti-α2 (1:400) subunit antibodies were used and were kindly provided by Dr. J.-M. Fritschy (Institute of Pharmacology, University of Zurich, Switzerland). These antibodies have been previously used for immunocytochemistry (Pirker et al., 2000). For the immunoperoxidase procedure, biotinylated anti-rabbit and anti-guinea pig IgG (H + L) from goat (1:200; Vector Laboratories) were used. Peroxidase enzyme activity was revealed using 3-3′-diaminobenzidine tetrahydrochloride (DAB, 0.5 mg/ml in 50 mM Tris–HCl buffer, pH 7.4; Sigma) as chromogen and 0.003% H_2O_2 as substrate. Reactions were stopped by rinsing the sections several times with TBS. Sections were then mounted onto gelatin–chromalum-coated slides, dehydrated and covered by coverslips.

2.6. In vitro slice preparation and electrophysiological recordings

Slices of the cerebellar vermis (Southan and Robertson, 1998) were obtained from male C57BL/6 (post-natal day (P) 19–35 days), and male and female γ2F77/F77 and γ2I77/I77 (P 18–35 and P 19–37 days, respectively) mice. Experiments on littermates of γ2F77/F77 and γ2I77/I77 mice from heterozygous breeding pairs were performed blind with regards to genotype. Mice were anaesthetised with isoflurane and decapitated, in accordance with the UK Animals (Scientific Procedures) Act 1986. The brains were rapidly removed, hemisected, and tissue blocks adhered to the cutting stage of a vibrotome (Leica VT1000s, Leica Microsystems, Vienna, Austria), and, for recordings from Purkinje cells, 300 μm sagittal slices were cut in ice-cold artificial cerebrospinal fluid (aCSF). The composition of the aCSF was (in mM): NaCl 126; $NaHCO_3$ 26; KCl 2.5; $CaCl_2$ 2; $MgCl_2$ 2; NaH_2PO_4 1.25; glucose 10; and kynurenic acid 3, final pH 7.3–7.4 when continuously oxygenated (95% O_2: 5% CO_2), adjusted with NaOH. For recordings from stellate and basket cells, 300 μm sagittal slices were cut in ice-cold aCSF of the above composition but with partial sucrose-substitution of the NaCl (NaCl 85; sucrose 73.6 mM). Slices for Purkinje cell recordings were stored for at least 1 h at room temperature in an incubation chamber containing the above continuously oxygenated aCSF, but without the kynurenic acid, and for stellate and basket cell recordings slices were initially stored in the sucrose aCSF for approximately 30 min before gradual replacement with normal aCSF, again without kynurenic acid. Slices for both sets of recordings were subsequently transferred to the recording chamber and perfused with warmed (33–34 °C, 1–2 ml/min) continuously oxygenated aCSF identical to that during cutting, and also containing 0.5 μM tetrodotoxin (TTX). All experiments typically took place within 7 h of slice preparation.

Purkinje or stellate and basket cells were visually identified using a Zeiss Axioskop (Zeiss, Oberkochen, Germany) equipped with infrared differential interference contrast optics with a 40× water immersion objective coupled to an infrared camera system (Hamamatsu, Hamamatsu City, Japan). Whole-cell patch-clamp recordings were made with an Axopatch 1D amplifier (Axon Instruments, Foster City, CA, USA). Patch pipettes for Purkinje cell recordings (tip resistance 2–3.5 MΩ) were pulled from borosillicate glass capillaries (GC120F-10, Harvard Apparatus, Kent, UK), and contained (in mM): KCl 140; $MgCl_2$ 1; $CaCl_2$ 1; Mg-ATP 4; Na-GTP 0.3; EGTA 10; HEPES 10, final pH ~7.30 adjusted with KOH, osmolality 294 mOsm. For recordings from stellate and basket cells pipettes (tip resistance 3–5 MΩ) contained (in mM): KCl 130; K-gluconate 10; $MgCl_2$ 2; Na_2-ATP 4; Na-GTP 0.3; EGTA 0.05; HEPES 10, final pH ~7.25 adjusted with KOH, osmolality 279 mOsm. Series resistance and whole-cell capacitance were monitored regularly during recording, and experiments were terminated if the series resistance changed by more than 25–30%. Series resistance was always compensated by ~80% using lag values of 6–8 μs. Experimental data were stored on digital audio tape for subsequent offline analysis.

The ionotropic glutamate receptor antagonist kynurenic acid was included in the aCSF during slice preparation to maintain slice viability, and in conjunction with TTX in the recording of aCSF to isolate

$GABA_A$ receptor-mediated mIPSCs. mIPSCs were recorded at a holding potential of −60 mV. The reversal potential of Cl^- was approximately 0 mV, therefore mIPSCs were inward. The effects of the BZ site agonists zolpidem (1 μM) and flurazepam (3 μM) on mIPSCs were examined after at least 5 min bath application of the drugs, although effects were already observable after 2–3 min. For some experiments, the BZ site antagonist flumazenil (10 μM) was bath applied following, and in the continuing presence of, 1 μM zolpidem, requiring combined application time longer than 10 min. The $GABA_A$ receptor antagonist 6-imino-3(4-methoxyphenyl)-1(6*H*)-pyridazinebutanoic acid (SR 95531) was either bath (50 μM) or focally (<50 μM) applied.

Stored data were digitised at 20 kHz using pClamp software via a DigiData 1200 analogue-to-digital converter (Axon Instruments), converted to an ASCII format, and detected and analysed using in-house, LabView based software (National Instruments, Austin, TX, USA) running on a personal computer (Jensen and Mody, 2001). Data were initially low pass filtered at 2 kHz, and mIPSCs were then detected using amplitude- (threshold typically 5–7 pA) and kinetics-based criteria. All identified events were confirmed by eye. Data were then imported into an analysis software, where populations of individual mIPSCs in a cell could be averaged. Averaged mIPSCs were calculated from at least 60 individual mIPSCs in a cell. The frequency of mIPSCs, and the peak amplitude, weighted decay, and 10–90% rise time of the averaged mIPSC were measured. The decay of the averaged mIPSC could be fit with a double exponential, and the weighted decay time constant was calculated using the following formula:

$$\tau_w = \tau_1 A_1 + \tau_2(1 - A_1)$$

where τ_w is the weighted decay time constant, τ_1 and τ_2 are the time constants of the first and second exponential functions, respectively, and A_1 is the proportion of the peak amplitude of the averaged mIPSC that is contributed by τ_1. The charge transfer for the averaged mIPSCs, the integrated area under each mIPSC, was calculated for each cell, as was the total current of mIPSCs. The effect of a drug on the frequency and total current of mIPSCs, and the parameters of the averaged mIPSC, was determined both in terms of absolute values and percent change. Statistical tests are as indicated in the text. The significance for comparison in all instances was set at $P < 0.05$. Statistical tests were performed using Excel, Statistica (Statsoft, Tulsa, OK, USA) or MatLab (Natick, MA, USA). In the text, all electrophysiological data are expressed as mean ± standard deviation.

Drugs for electrophysiological experiments were obtained from the following sources: kynurenic acid and flurazepam, Sigma Chemicals, UK; TTX, SR 95531, zolpidem and flumazenil, Tocris, Bristol, UK. Zolpidem and flumazenil were initially dissolved in dimethyl sulfoxide (DMSO) before addition to the aCSF. For 1 μM zolpidem, the final concentration of DMSO in the bath was 1:10,000–1:100,000. For experiments involving application of 1 μM zolpidem followed by application of 10 μM flumazenil in the continuing presence of 1 μM zolpidem, the final concentration of DMSO was <1:9000. Flurazepam, TTX and SR 95531 were dissolved initially in distilled water before addition to the aCSF. Kynurenic acid was dissolved directly into the aCSF.

2.7. Behavioural studies

Male and female C57BL/6, γ2F77/F77 and γ2I77/I77 mice (3–5 months of age weighing 20–38 g at the beginning of experiments) were maintained at the Central Animal Laboratory (University of Turku, Turku, Finland) in groups of 4–12 in polypropylene Macrolon cages in a room artificially illuminated from 7 a.m. to 7 p.m. and air-conditioned (20 ± 1 °C, relative humidity of 50 ± 10%). Tap water and pellets were available ad libitum. All experimental protocols were approved by the Institutional Animal Care and Use Committee of the University of Turku. Due to obvious differences in the fur colour of the mouse strains, behavioural tests were carried out in a randomised, but not blind, fashion by several observers, each taking the responsibility of a complete experiment. All animal groups consisted of about equal numbers of female and male mice, and all the data are pooled for the genders since they did not show any significant gender differences in these tests for any of the mouse lines. Examination of various behavioural and physiological properties of the mouse lines was performed using a modified version of the primary screen of SHIRPA protocol (Rogers et al., 1999).

In a staircase test for measuring exploratory behaviour and locomotion, the mice were placed individually for 3 min in a wooden box, which consisted of five steps (2.5 cm high, 10 cm wide, 7.5 cm deep) surrounded by a 12.5 cm high wall (Jones et al., 1997). The animals were treated either with saline (1 ml/kg i.p.) or with 3 mg/kg zolpidem tartrate (Synthelabo Recherche, Bagneux, France). Thirty minutes after the injections, the mice were placed on the lowest step facing away from the ascending steps. The number of steps climbed up (all four paws on the next step) were counted. All the mice were naïve to drugs and test environment.

In a rotarod test, the ability of mice to stay on an accelerating rotating rod (Rotamex 4/8, Columbus Instruments, Columbus, OH, USA) was used to assess motor performance and drug-induced motor impairment (Jones et al., 1997). The mice were first trained to

stay on a stationary rod, and then on a rod rotating evenly at a speed of 3.5 rpm for 90 s. In learning trials, the mice were initially placed on a non-moving rod, the rotation was then immediately started at 3.5 rpm, and thereafter gradually increased to 17.5 rpm over a 180 s measuring interval. The time for which the mice were able to stay on the rod was recorded. The effects of zolpidem tartrate and flurazepam dihydrochloride (Sigma) were then tested on these animals using a cumulative dosing paradigm (1, 3, 10 and 30 mg/kg i.p. for zolpidem; 10, 20, 30 and 40 mg/kg i.p. for flurazepam). In groups of four mice, the experiments were started with saline injections, followed 15 min later by three or four test trials on the rotarod. This was followed immediately by the first drug administration. Further rotarod tests then ensued 15 min later, and so on, until the last injection to obtain the final cumulative dose. Animals used for this test had at least 5 days and one injection-free trial on the rotarod between the drug experiments.

Statistical tests, as indicated in the text, used to assess the significance of differences between the mouse lines, test trials, drug treatments and interactions, were performed using Prism 2.0 program (GraphPad Software). The significance for comparison in all instances was set at $P < 0.05$. Data are presented as mean ± standard deviation.

3. Results

We generated the F77I point mutation in the mouse γ2 $GABA_A$ receptor subunit gene by homologous recombination in embryonic stem cells (Fig. 1). The resulting mice were healthy and viable. They bred normally and behaved similarly to control C57BL/6 and γ2F77/F77 mice when examined with a range of standard behavioural observational tests (SHIRPA protocol; data not shown), indicating that the point mutation did not cause any changes in general behaviour or physiology of these mice. The overall structure and cellular architecture of the brains also appeared normal (data not shown). We examined the effect of the γ2F77I mutation on $GABA_A$ receptor levels and pharmacology in the cerebellum, a brain region with a high expression density of γ2 subunit in α1β2/3γ2 subunit containing receptors (Wisden et al., 1992, 1996).

3.1. The expression of $GABA_A$ receptors in the cerebellum of γ2I77/I77 mice

Using quantitative western blot analysis, we compared the expression of $GABA_A$ receptor subunits between cerebella of γ2F77/F77 and γ2I77/I77 mice. Table 1 shows that there was no difference in expression levels of the α1, α6, β2, β3 and δ subunits between the γ2F77/F77 and γ2I77/I77 mice. However, the γ2 subunit levels were, on average, 15% lower (unpaired *t*-test) in the whole cerebellum of γ2I77/I77 mice.

Table 1
Evaluation of $GABA_A$ receptor subunit expression in cerebella of γ2F77/F77 and γ2I77/I77 mice by western blot analysis. Data are presented as mean ± standard deviation. n = number of individual animals tested (see Materials and methods for details). Significant differences between genotypes are highlighted in italics ($P < 0.05$ Student's unpaired *t*-test)

Subunit	γ2F77/F77		γ2I77/I77	
	Percentage of $GABA_A$ receptors	n	Percentage of $GABA_A$ receptors	n
α_1	100.0 ± 8.6	6	95.0 ± 3.5	5
α6	101.3 ± 7.2	6	92.6 ± 5.0	5
β2	100.0 ± 4.3	6	112.3 ± 4.2	5
β3	100.5 ± 1.7	6	110.3 ± 5.6	5
γ2	101.3 ± 5.2	6	*86.7±2.4*	5
δ	100.1 ± 5.1	6	89.6 ± 2.6	5

The distribution of the $GABA_A$ receptor subunits in the brains of γ2I77/I77 and γ2F77/F77 mice was further studied by immunocytochemistry. No detectable differences in either the distribution or the intensity of immunoreactivity for the γ2 subunit were observed in any layer of the cerebellar cortex (Fig. 2), or in the deep cerebellar nuclei (data not shown). We also investigated the distribution of immunoreactivity for α1, α2 and β3 subunits, which are prominently expressed in the cerebellum (Wisden et al., 1996; Pirker et al., 2000). For all these $GABA_A$ receptor subunits, no changes were detected in either the pattern or intensity of immunoreactivity in the cerebellar cortex and deep nuclei between the two mouse genotypes (Fig. 2). Immunolabelling for the $GABA_A$ receptor subunits in both the γ2I77/I77 and γ2F77/F77 mice was similar to that described in the rat (Pirker et al., 2000).

The number of $GABA_A$ receptors in the cerebellum of both γ2F77/F77 and γ2I77/I77 mice was determined by calculating both the solubilisation efficiency and total number of [^{3}H]muscimol (40 nM) binding sites. Neither the solubilisation efficiency (83.1 ± 2.0% and 84.0 ± 1.6%, respectively), nor the total number of binding sites of either the supernatant extract (3.3 ± 1.0 and 3.0 ± 0.9 pmol/mg) or the re-dissolved pellet (0.7 ± 0.1 and 0.6 ± 0.1 pmol/mg) obtained by centrifugation at $150,000 \times g$, were significantly different between genotypes (unpaired *t*-test). Western blot analysis performed in the supernatant extract and re-dissolved pellet showed no significant difference in the extraction efficacy of the α1, α6, γ2 or δ subunits between γ2F77/F77 and γ2I77/I77 cerebella, indicating that the major $GABA_A$ receptor subtypes were extracted to a similar extent under the experimental conditions used (data not shown). The total amounts of

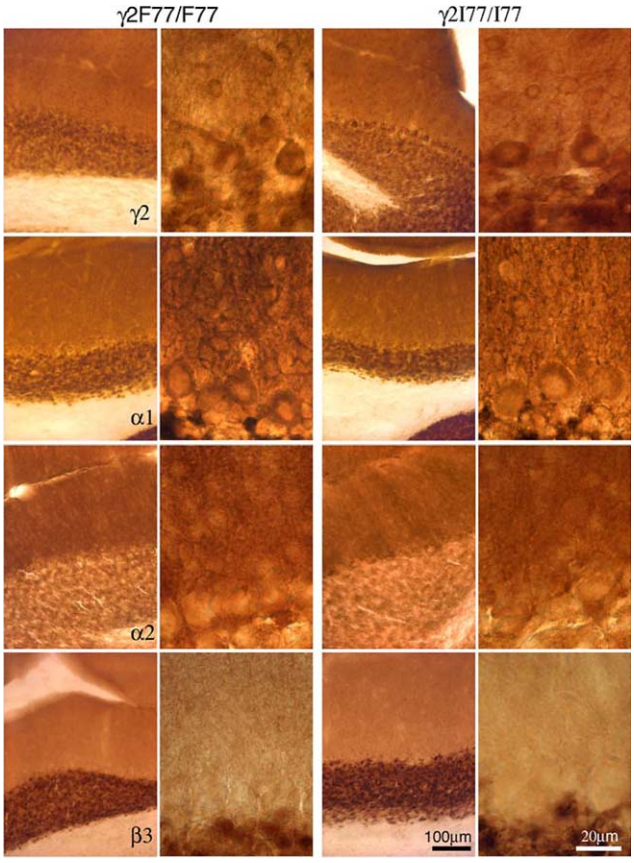

Fig. 2. Immunocytochemical comparison of $GABA_A$ receptor subunit distribution in cerebellar cortex of γ2F77/F77 and γ2I77/I77 mice. First and third columns show low power light micrographs, second and fourth columns show cellular details at higher magnification. Immunoreactivity for the γ2, α1, α2 and β3 $GABA_A$ receptor subunits in sections of the cerebellar cortex of γ2F77/F77 and γ2I77/I77 mice showed no obvious differences. Scale bars apply to the first and third, or to the second and fourth columns, respectively.

α1, α6, and δ subunits present in the pellet plus supernatant were comparable in the cerebella of γ2F77/F77 and γ2I77/I77 mice, but the total amounts of γ2 subunits were reduced to 92% in cerebella of γ2I77/I77 mice, in agreement with the data presented in Table 1.

3.2. *The potency of zolpidem for the inhibition of [^{3}H]flunitrazepam binding is decreased in γ2I77/I77 mice*

We compared the inhibition of [^{3}H]flunitrazepam binding by zolpidem, flumazenil and flurazepam in adult cerebella of γ2F77/F77 ($n = 3$ animals) and γ2I77/I77 ($n = 3$ animals) mice. The potency of zolpidem for the inhibition of [^{3}H]flunitrazepam (5 nM) binding was strongly reduced in γ2I77/I77 mice, compared to γ2F77/F77 mice (Fig. 3A). The EC_{50} of zolpidem was 33.7 nM for γ2F77/F77 mice, and 17.4 μM for γ2I77/I77 mice. The potency of flumazenil for inhibition of [^{3}H]flunitrazepam binding was also dramatically decreased in γ2I77/I77 compared to γ2F77/F77 mice (Fig. 3B). The EC_{50} of flumazenil was 2.9 nM for γ2F77/F77 mice, and 1.8 μM for γ2I77/I77 mice. For both zolpidem and flumazenil, this decrease was seen as a large shift to the right in the inhibition of [^{3}H]flunitrazepam binding curves (Fig. 3A and B). The potency of flurazepam for inhibition of [^{3}H]flunitrazepam binding was reduced to a much lesser degree

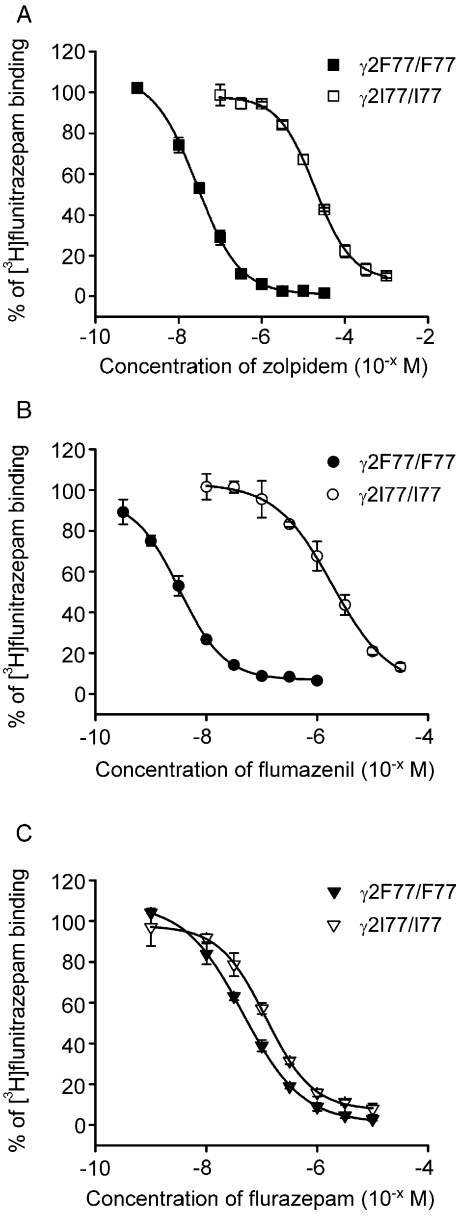

Fig. 3. Potency of zolpidem (A), flumazenil (B), and flurazepam (C) for the inhibition of [^{3}H]flunitrazepam binding in cerebellar membranes of γ2F77/F77 (filled symbols) and γ2I77/I77 (open symbols) mice. Note that the γ2F77I point mutation dramatically shifts the curves for zolpidem and flumazenil to the right, indicating a decrease in potency, whereas that for flurazepam is little affected. Data shown are mean ± standard deviation from a single experiment performed in triplicate. The experiments were performed twice with comparable results.

than that of either zolpidem or flumazenil, although there was still a small shift to the right in the binding curve (Fig. 3C). The EC_{50} for flurazepam was 54.8 nM for γ2F77/F77 mice, and 111.2 nM for γ2I77/I77 mice. We also tested whether the binding of [^{3}H]flunitrazepam itself was altered by the point mutation. In cerebella of γ2I77/I77 mice, the affinity of [^{3}H]flunitrazepam binding was significantly (unpaired *t*-test) decreased to $K_d = 9.6 \pm 0.3$ nM compared to $K_d = 5.4 \pm 0.7$ nM in cerebella of γ2F77/F77 mice ($n = 3$ experiments). The B_{max} was not different between the two genotypes (γ2F77/F77 2.8 ± 0.2 pmol/mg; γ2I77/I77 3.1 ± 0.2 pmol/mg). Thus, the γ2F77I point mutation reduces the binding of selected BZ site ligands, as described previously using heterologous expression of receptors (Buhr et al., 1997; Wingrove et al., 1997).

3.3. Comparison of mIPSCs in Purkinje cells of mice with different genetic background

Control mIPSCs recorded prior to drug application were compared in order to assess potential differences in synaptic currents caused either by the point mutation or genetic background. Control mIPSCs in cells from γ2I77/I77, γ2F77/F77 and C57BL/6 mice were recorded in the presence of kynurenic acid (3 mM) and TTX (0.5 μM) (Fig. 4A), and were similar to previously described recordings in both the rat (Llano and Marty, 1995) and mouse (Southan and Robertson, 1998; Zhang et al., 1999). The peak amplitude of the averaged mIPSCs was -56.31 ± 15.99 pA in C57BL/6 mice ($n = 42$ cells from 13 mice), -57.24 ± 16.71 pA in γ2F77/F77 mice ($n = 50$ cells from 14 mice), and -54.55 ± 19.57 pA in γ2I77/I77 mice ($n = 40$ cells from 13 mice) (Fig. 4B). These values were not significantly different from each other (ANOVA). The weighted decay of the averaged mIPSCs was significantly shorter in the γ2I77/I77 mice (2.36 ± 0.35 ms) compared to both the C57BL/6 (2.72 ± 0.41 ms) and γ2F77/F77 mice (2.75 ± 0.54 ms, $P < 0.05$, ANOVA with post hoc Tukey HSD) (Fig. 4B). The weighted decay of the averaged mIPSCs in the C57BL/6 and γ2F77/F77 mice was not significantly different from each other. In addition, the charge transfer of the averaged mIPSC was significantly smaller in γ2I77/I77 (-144.23 ± 76.65 fC) mice compared to γ2F77/F77 (-181.22 ± 69.32 fC), but not C57BL/6, mice (-177.92 ± 60.13 fC) (Fig. 4B). The 10–90% rise times of the averaged mIPSCs were not significantly different between the three groups (C57BL/6 306.91 ± 25.33 μs, γ2F77/F77 304.60 ± 28.37 μs, γ2I77/I77 305.75 ± 25.71 μs), nor was the frequency of mIPSCs (C57BL/6 10.21 ± 7.37 Hz, γ2F77/F77 10.85 ± 7.50 Hz, γ2I77/I77 10.26 ± 9.75 Hz), or the total current of mIPSCs between groups of

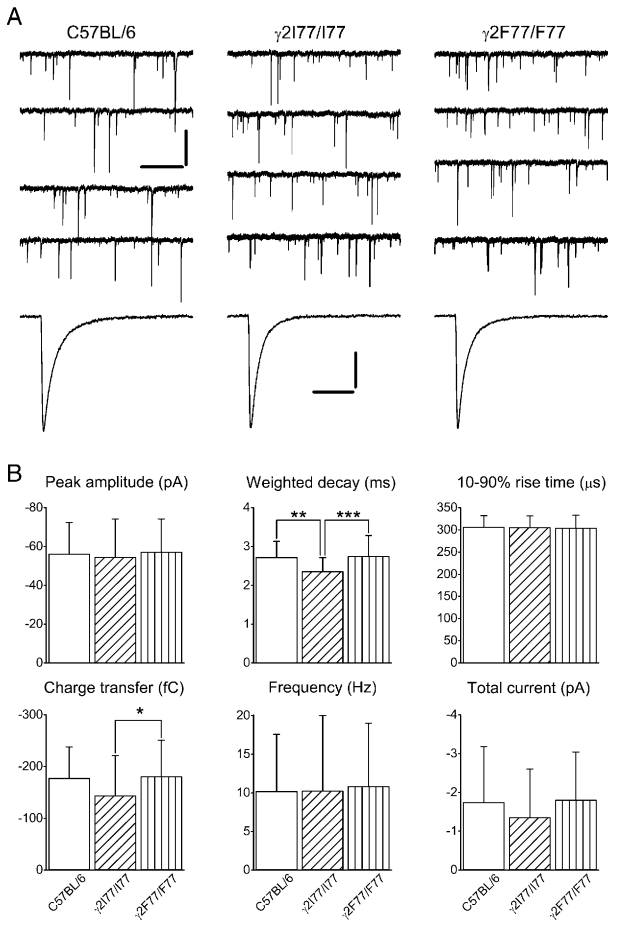

Fig. 4. Comparison of mIPSCs in Purkinje cells of C57BL/6, γ2I77/I77 and γ2F77/F77 mice. (A) Four consecutive traces showing mIPSCs from a Purkinje cell of a P19 C57BL/6 mouse (left panel), P24 γ2I77/I77 mouse (middle panel), and P30 γ2F77/F77 mouse (right panel). Recordings for this and subsequent electrophysiology figures were performed in the presence of kynurenic acid (3 mM) and TTX (0.5 μM). Lowest traces show the waveforms of the averaged mIPSCs for the cells above; (B) Comparison of mIPSC parameters between genotypes for all recorded cells (C57BL/6, $n = 42$, white bars; γ2I77/I77 $n = 40$, diagonally lined bars; γ2F77/F77 $n = 50$, vertically lined bars). Data for the peak amplitude, weighted decay, 10–90% rise time and charge transfer are obtained from the averaged mIPSCs, frequency and total current from all mIPSCs. Data presented here, and for all subsequent figures, are mean ± standard deviation. * indicates $P < 0.05$, ** $P < 0.01$ and *** $P < 0.001$, ANOVA with post hoc Tukey HSD. Calibration bars, A upper panels, 500 ms and 100 pA; lower panels, 10 ms and 20 pA.

animals (C57BL/6 -1.75 ± 1.43 pA, γ2F77/F77 -1.81 ± 1.23 pA, γ2I77/I77 -1.36 ± 1.24 pA) (Fig. 4B), probably reflecting the large variation in frequency of mIPSCs within and between mice with different genotype.

The $GABA_A$ receptor antagonist SR 95531 (≤50 μM) completely blocked mIPSCs in Purkinje cells of γ2F77/F77 ($n = 4$ cells) and γ2I77/I77 ($n = 3$ cells) mice, confirming they were mediated by $GABA_A$ receptors (data not shown).

3.4. Zolpidem does not potentiate mIPSCs in Purkinje cells of γ2I77/I77 mice

Bath application of the BZ site agonist zolpidem (1 μM) to Purkinje cells of C57BL/6 and γ2F77/F77 mice caused a robust and reliable potentiation of the mIPSCs (Fig. 5), as described previously for a variety of other cells (e.g. De Koninck and Mody, 1994; Perrais and Ropert, 1999; Hájos et al., 2000). In cells of both C57BL/6 ($n = 25$ cells from 11 mice) and γ2F77/F77 ($n = 25$ cells from 11 mice) mice, zolpidem caused a significant (Student's paired t-test) increase in the peak amplitude, weighted decay, 10–90% rise time, charge transfer of the averaged mIPSCs, and total current of mIPSCs. The frequency of mIPSCs was significantly increased in γ2F77/F77 mice, but not in C57BL/6 mice (Fig. 5A and C and Table 2). By comparison, in γ2I77/I77 mice, zolpidem did not significantly alter the peak amplitude, weighted decay, 10–90% rise time or charge transfer of the averaged mIPSCs, or the total current and frequency of mIPSCs ($n = 16$ cells from eight mice) (Fig. 5B, and Table 2). We calculated the percent change in each parameter and compared them between the three genotypes. In C57BL/6 and γ2F77/F77 mice, zolpidem increased peak amplitude, weighted decay, 10–90% rise time and charge transfer of the averaged mIPSC, and also the total current of mIPSCs, to a greater degree than in γ2I77/I77 mice (Kruskal–Wallis test with post hoc Dunn) (Fig. 5D and E and Table 2). Changes were never different between C57BL/6 and γ2F77/F77 mice. Any changes in frequency were not different between the three genotypes. Therefore, the γ2F77I point mutation completely abolished the potentiation of mIPSCs by 1 μM zolpidem in Purkinje cells, which probably express only α1 subunit containing receptors (Wisden et al., 1992, 1996).

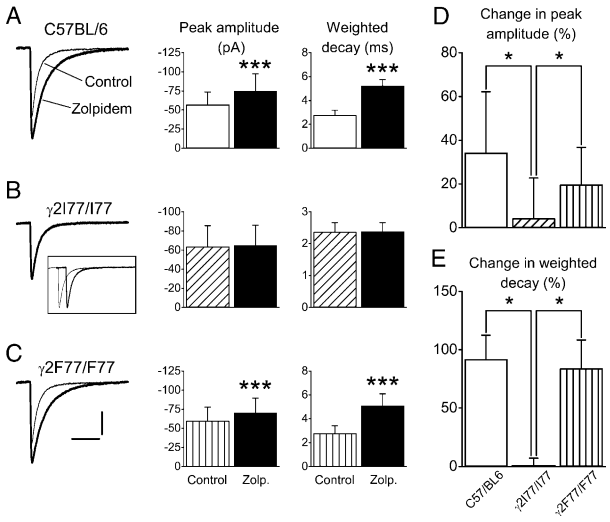

Fig. 5. Effects of zolpidem on Purkinje cell mIPSCs from the three mouse genotypes. (A–C) Left panels, waveforms of the averaged mIPSC in the absence (thin line) and in the presence of zolpidem (1 μM, thick line), for Purkinje cells of a P19 C57BL/6 mouse, P28 γ2I77/I77 mouse and P30 γ2F77/F77 mouse. Zolpidem caused a large increase in both peak amplitude and decay of the averaged mIPSC in the cells from the C57BL/6 and γ2F77/F77 mice, but had no effect on mIPSCs of the cell from the γ2I77/I77 mouse. The similarity of the traces can be seen in the inset. Middle and right panels, graphs showing the increase caused by zolpidem (black bars, *** indicates $P < 0.001$, Student's paired t-test) in peak amplitude and weighted decay for all cells from C57BL/6 ($n = 25$) and γ2F77/F77 ($n = 25$) mice, but not in γ2I77/I77 mice ($n = 16$). (D–E) Graphs showing the mean percent increase in peak amplitude and weighted decay for all recorded cells from C57BL/6 (white bar), γ2I77/I77 (diagonally lined bar) and γ2F77/F77 mice (vertically lined bar). * indicates $P < 0.05$, Kruskal–Wallis test with post hoc Dunn. Calibration bars in (A–C), 10 ms and 20 pA.

Table 2
Actions of 1 μM zolpidem on mIPSC properties in Purkinje cells of C57BL/6, γ2I77/I77 and γ2F77/F77 mice. Data are presented as mean ± standard deviation. Percent change in each parameter was calculated for each cell and then averaged. Only significant differences within, not between, genotypes are highlighted in italics ($P < 0.05$, Student's paired t-test)

mIPSC parameter	Experimental condition	Mouse genotype					
		C57BL/6 ($n = 25$)		γ2I77/I77 ($n = 16$)		γ2F77/F77 ($n = 25$)	
		Absolute data	Percent change	Absolute data	Percent change	Absolute data	Percent change
Peak amplitude (pA)	Control	−56.9 ± 16.7	34.3 ± 27.9	−63.8 ± 21.7	4.3 ± 18.4	−59.8 ± 18.0	19.8 ± 16.9
	+1 μM Zolp	*−74.9±22.5*		−65.1 ± 20.8		*−70.4±19.1*	
Weighted decay (ms)	Control	2.8 ± 0.4	91.8 ± 20.6	2.4 ± 0.3	1.0 ± 6.0	2.8 ± 0.6	84.0 ± 24.3
	+1 μM Zolp	*5.2±0.5*		2.4 ± 0.3		*5.1±1.0*	
10-–90% rise time (μs)	Control	304.0 ± 29.4	11.6 ± 7.8	298.8 ± 20.0	0.7 ± 5.0	299.6 ± 23.7	12.3 ± 6.6
	+1 μM Zolp	*338.0±28.0*		300.6 ± 23.0		*336.8±34.6*	
Charge transfer (fC)	Control	−185.0 ± 64.7	144.8 ± 62.7	−163.6 ± 106.9	−7.5 ± 51.2	−192.5 ± 83.5	113.3 ± 47.4
	+1 μM Zolp	*−438.6±163.8*		−181.9 ± 67.9		*−392.5±134.5*	
Frequency (Hz)	Control	8.4 ± 5.5	12.3 ± 36.0	8.5 ± 6.4	21.7 ± 61.8	12.1 ± 8.1	14.9 ± 26.4
	+1 μM Zolp	8.9 ± 5.5		9.3 ± 6.4		*13.5±8.6*	
Total current (pA)	Control	−1.49 ± 1.11	179.4 ± 122.2	−1.46 ± 1.24	10.9 ± 92.9	−2.06 ± 1.29	144.2 ± 81.7
	+1 μM Zolp	*−4.17±3.94*		−1.70 ± 1.49		*−5.06±3.44*	

3.5. The BZ site antagonist flumazenil reverses the actions of zolpidem in Purkinje cells of C57BL/6 and γ2F77/F77 mice

In a subset of Purkinje cells from the three genotypes, the BZ site antagonist flumazenil (10 μM) was applied following, and in the continuing presence of, zolpidem (1 μM), to test whether the observed effects of zolpidem had been caused by its action at the BZ binding site. In the C57BL/6 mice ($n = 7$ cells from five mice) flumazenil significantly (Mann–Whitney *U*-test) reversed increases in peak amplitude, weighted decay, 10–90% rise time and charge transfer back to control values (Fig. 6A, D and E). Similarly, in γ2F77/F77 mice ($n = 6$ cells from three mice), flumazenil significantly reversed increases in peak amplitude, weighted decay and charge transfer back to control values (Fig. 6C–E). In all instances, mIPSC parameter values following flumazenil application in the continuing presence of zolpidem were similar to control values. In Purkinje cells of γ2I77/I77 mice ($n = 6$ cells from three mice), the mIPSC parameters in the presence of zolpidem, and in the presence of flumazenil in the continuing presence of zolpidem, were not significantly different from the control values (ANOVA, Fig. 6B, D and E). The frequency and total current of mIPSCs in the three genotypes in the presence of zolpidem, and flumazenil in the continuing presence of zolpidem, were not different from control. Therefore all observed effects of zolpidem in Purkinje cells of C57BL/6 and γ2F77/F77 mice were mediated by its action at the BZ binding site of the $GABA_A$ receptor.

3.6. The effects of flurazepam are unaltered in Purkinje cells of γ2I77/I77 mice

In order to test the selectivity of the γ2F77I point mutation for zolpidem, we examined the effects of another BZ site agonist, flurazepam, on the Purkinje cell mIPSCs, the binding of which remains largely unaffected by the γ2F77I point mutation (Fig. 3; see also Buhr et al., 1997; Wingrove et al., 1997). Bath application of flurazepam (3 μM) caused a significant increase (Student's paired *t*-test) in the peak amplitude, weighted decay and charge transfer of the averaged mIPSCs in all three genotypes (C57BL/6 $n = 5$ cells from two mice; γ2F77/F77 $n = 7$ cells from two mice; γ2I77/I77 $n = 5$ cells from three mice) (Fig. 7). In γ2F77/F77 and γ2I77/I77 mice, flurazepam also caused a small, but significant, increase in 10–90% rise time, but not in C57BL/6 mice. Flurazepam caused a significant increase in total current of mIPSCs only in γ2F77/F77 mice. Frequency was unaltered in all three genotypes. Flurazepam increased peak amplitude $24.19 \pm 9.81\%$ in C57BL/6 mice, $20.78 \pm 8.97\%$ in γ2F77/F77 mice, and $24.68 \pm 25.74\%$ in γ2I77/I77 mice (Fig. 7D). Weighted decay increased $49.70 \pm 17.43\%$ in C57BL/6 mice, $49.82 \pm 10.21\%$ in γ2F77/F77 mice, and $44.35 \pm 12.41\%$ in γ2I77/I77 mice (Fig. 7E). Finally, charge transfer increased $81.60 \pm 29.85\%$ in C57BL/6 mice, $77.32 \pm 27.73\%$ in γ2F77/F77 mice, and $75.19 \pm 27.81\%$ in γ2I77/I77 mice. The increases in each parameter were not significantly different between genotypes (Kruskal–Wallis test). In addition, changes in the other mIPSC parameters were not different between the three genotypes (data not shown). The increases in mIPSC parameters

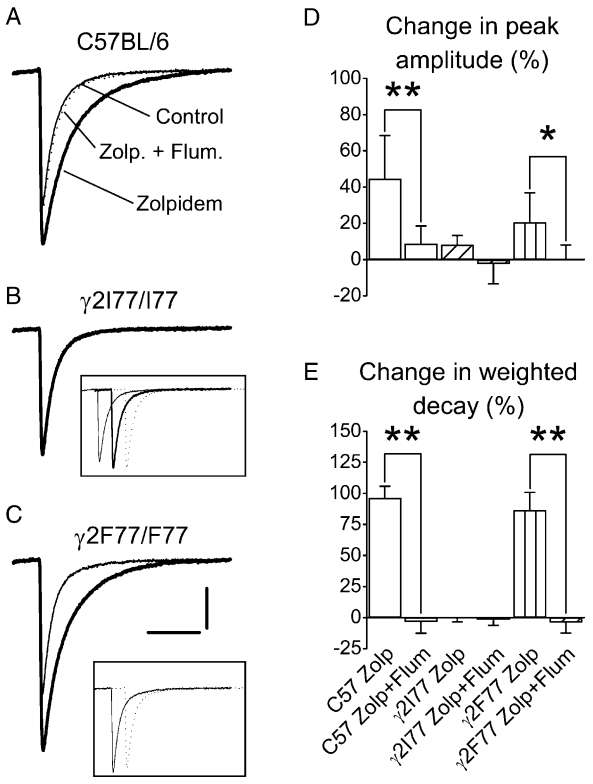

Fig. 6. Effects of flumazenil application in the continuing presence of zolpidem on Purkinje cell mIPSCs. (A–C) Waveforms of the averaged mIPSC for individual Purkinje cells from a P28 C57BL/6 mouse, P21 γ2I77/I77 mouse, and P23 γ2F77/F77 mouse, during control (thin line), following zolpidem (1 μM) application (thick line), and following flumazenil (10 μM) application in the continuing presence of zolpidem (dotted line). In the cell from the C57BL/6 mouse, flumazenil reverses the increases in peak amplitude and decay caused by zolpidem, so that the control and flumazenil traces are similar. In the cell from the γ2F77/F77 mouse, flumazenil reverses the action of zolpidem completely so that the control and flumazenil traces overlap. The similarity can be seen in the inset. In the cell from the γ2I77/I77 mouse, zolpidem and flumazenil in the presence of zolpidem had no effect on peak amplitude and decay, so that all three traces overlap. Similarity of the three traces can be seen in the inset. (D–E) Graphs showing the mean percent change in peak amplitude and weighted decay caused by application of zolpidem and flumazenil in the continuing presence of zolpidem for all cells from C57BL/6 ($n = 7$), γ2I77/I77 ($n = 6$) and γ2F77/F77 ($n = 6$) mice. Flumazenil reversed the increases in peak amplitude and weighted decay in C57BL/6 and γ2F77/F77 mice (* indicates $P < 0.05$ and ** $P < 0.01$, Mann–Whitney *U*-test). Calibration bars in (A–C), 10 ms and 20 pA.

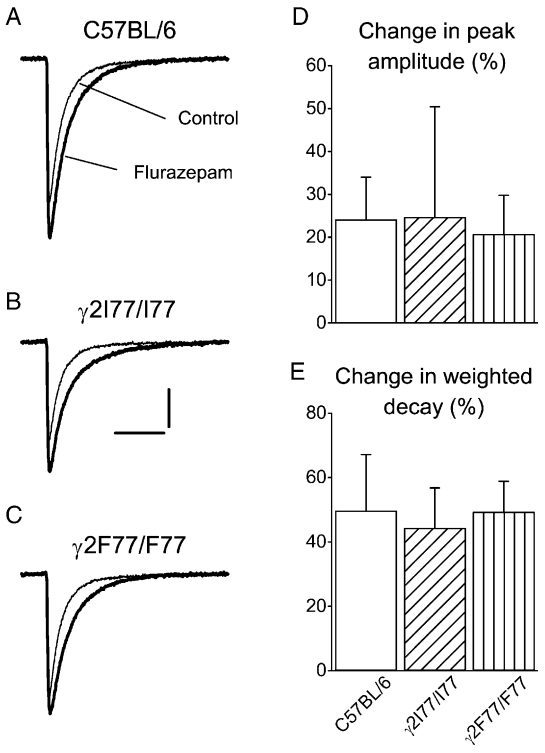

Fig. 7. Effects of flurazepam on Purkinje cell mIPSCs. (A–C) Waveforms of the averaged mIPSCs before (thin line) and following the application of flurazepam (3 μM, thick line) for a Purkinje cell of a P26 C57BL/6 mouse, P34 γ2I77/I77 mouse and P31 γ2F77/F77 mouse. Flurazepam caused an increase in peak amplitude and decay in all three cells. (D–E) Graphs showing comparison of the mean percent increase in peak amplitude and weighted decay for all cells from C57BL/6 ($n = 5$, white bars), γ2I77/I77 ($n = 5$, diagonally lined bars) and γ2F77/F77 ($n = 7$, vertically lined bars) mice. There was no significant difference between genotypes ($P > 0.05$, Kruskal–Wallis test). Calibration bars in (A–C), 10 ms and 20 pA.

were smaller than those observed following the application of zolpidem (see above). Thus, the effects of flurazepam were virtually indistinguishable between the three genotypes, and confirm the selectivity of the γ2F77I point mutation for zolpidem.

3.7. *Effects of zolpidem on mIPSCs in cerebellar stellate/basket cells*

In order to test if the γ2F77I point mutation produced similar effects in other cell types, we recorded mIPSCs from cerebellar stellate and basket cells from γ2F77/F77 and γ2I77/I77 mice, and examined the effects of zolpidem application. Since cerebellar stellate and basket cells exhibit similar synaptic properties and express similar $GABA_A$ receptor subunits (Llano and Marty, 1995; Wisden et al., 1996; Southan and Robertson, 1998), no attempt was made to differentiate the two types of molecular layer interneurones.

The values of mIPSC parameters in stellate/basket cells under control conditions between the two groups of mice were not significantly different (γ2F77/F77 $n = 8$ cells from four mice; γ2I77/I77 $n = 9$ cells from three mice, unpaired t-test) and were similar to those observed in previous studies (Llano and Marty, 1995; Nusser et al., 1997; Southan and Robertson, 1998; Vicini et al., 2001). Peak amplitude was -60.55 ± 13.33 and -63.92 ± 12.22 pA; weighted decay 3.22 ± 0.67 and 3.34 ± 0.34 ms; 10–90% rise time 286.67 ± 21.21 and 307.50 ± 36.15 μs; charge transfer -226.62 ± 64.89 and -247.13 ± 47.83 fC; frequency 1.13 ± 0.51 and 2.43 ± 2.20 Hz; and total current of mIPSCs -0.24 ± 0.92 and -0.67 ± 0.67 pA, in γ2I77/I77 and γ2F77/F77 mice, respectively.

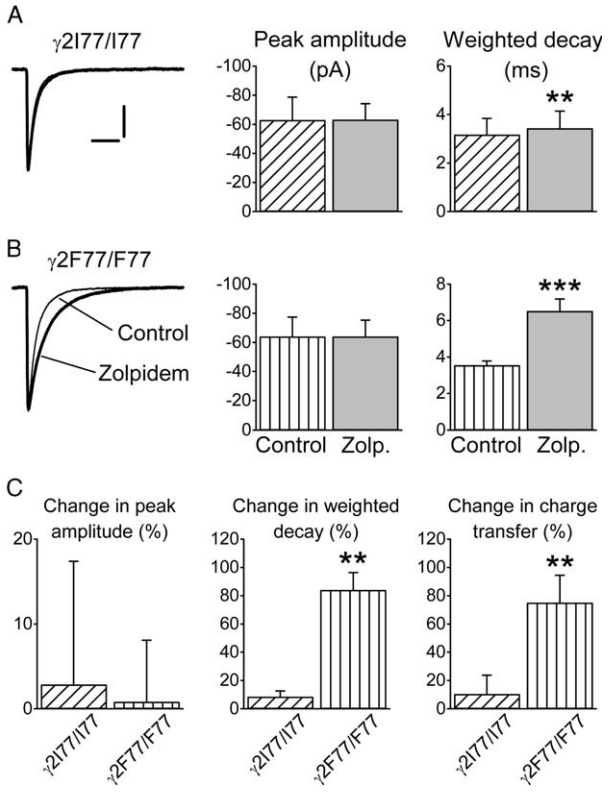

Fig. 8. Actions of zolpidem on mIPSCs in stellate/basket cells. (A, B) Left panels: waveforms of the averaged mIPSCs before (thin line) and following the application of zolpidem (1 μM, thick line) for a stellate/basket cell of a P37 γ2I77/I77 mouse and P25 γ2F77/F77 mouse. Zolpidem caused a large increase in weighted decay but no increase in peak amplitude in the cell from a γ2F77/F77 mouse and a small increase in weighted decay but no increase in peak amplitude in the cell from a γ2I77/I77 mouse. Middle and right panels: graphs showing the change in peak amplitude and weighted decay caused by zolpidem (grey bars) from all recorded cells (γ2I77/I77 $n = 5$, γ2F77/F77 $n = 5$). Zolpidem caused a significant increase in weighted decay (** indicates $P < 0.01$ and *** $P < 0.001$, Student's paired t-test), but not peak amplitude, for both genotypes. (C) Graphs showing comparison of percent increase in peak amplitude, weighted decay and charge transfer of the averaged mIPSC for all cells from γ2I77/I77 (diagonally lined bars) and γ2F77/F77 (vertically lined bars) mice. ** indicates $P < 0.01$, Mann–Whitney U-test. Calibration bars in A and B, 10 ms and 20 pA.

In stellate/basket cells of γ2F77/F77 mice ($n = 5$ cells from four mice), zolpidem significantly (Student's paired *t*-test) increased weighted decay, 10–90% rise time and charge transfer of the averaged mIPSC, but there was no change in the peak amplitude (Fig. 8C–E, and Table 3). In γ2I77/I77 mice ($n = 5$ cells from two mice), zolpidem caused a small, but significant ($8.6 \pm 3.9\%$) increase in weighted decay, but not in any other parameter (Fig. 8B, and Table 3). Zolpidem did not significantly change the frequency or total current of mIPSCs in either genotype (Table 3). The increases in weighted decay and charge transfer were significantly larger in the γ2F77/F77 mice than in the γ2I77/I77 mice (Mann–Whitney *U*-test) (Fig. 8D and E).

Therefore, in contrast to the Purkinje cells, the γ2F77I point mutation does not completely abolish zolpidem potentiation of mIPSCs in stellate/basket cells, as it caused a small increase in the weighted decay in the γ2I77/I77 mice.

3.8. Point mutant γ2I77/I77 mice are behaviourally insensitive to zolpidem

We tested the sensitivity of γ2I77/I77 mice to zolpidem behaviourally using a test of simple exploratory activity, the staircase test. Control experiments using an i.p. injection of saline showed no differences between the three genotypes. C57BL/6 mice ($n = 8$ animals) climbed 17.71 ± 3.25 stairs, γ2I77/I77 mice ($n = 8$) 14.57 ± 3.53 stairs and γ2F77/F77 mice ($n = 3$) 8.67 ± 4.37 stairs (Fig. 9A). Point mutant γ2I77/I77 mice receiving a moderate dose of zolpidem (3 mg/kg i.p.) showed a strong resistance to its action, exhibiting similar exploratory activity (13.86 ± 3.78 stairs climbed, $n = 7$ animals) to that observed following saline injection. However, both C57BL/6 and γ2F77/F77 mice were clearly affected (Fig. 9A). Zolpidem sedated these mice so effectively that they failed to explore the stairs at all (C57BL/6 mice, 0 stairs climbed, $n = 7$ animals; γ2F77/F77 mice, 1.20 ± 0.97 stairs, $n = 5$ animals).

These observations were extended to examine motor performance using a rotarod test, which has a known cerebellar contribution. The γ2I77/I77 mice were also insensitive to zolpidem on this test. Cumulative zolpidem injections (1–30 mg/kg i.p., animals tested 15 min after injections) increasingly affected C57BL/6 ($n = 5$ animals) and γ2F77/F77 ($n = 6$ animals) mice so that at the highest dose these mice could not stay on the rotarod (Fig. 9B). By contrast, in the γ2I77/I77 mice ($n = 13$ animals), motor function appeared to be completely unaffected, and these mice were able to stay on the rotarod for the full duration of the test period (Fig. 9B). The time spent on the rotarod by C57BL/6 and γ2F77/F77 mice was significantly shorter compared to γ2I77/I77 mice for all doses of zolpidem tested (ANOVA with post hoc Newman–Keuls), but the saline injection produced no difference.

To further test the selectivity of the γ2F77I point mutation for zolpidem, cumulative doses of flurazepam (10–40 mg/kg i.p.) were administered to C57BL/6 ($n = 5$ animals) and γ2I77/I77 ($n = 10$ animals) mice (no γ2F77/F77 mice were available for this experiment), and the animals were tested on the rotarod 15 min after drug injection. High doses of flurazepam caused a similar decrease in the ability of the mice from both genotypes to stay on the rotarod (Fig. 9C). Differences between the genotypes were not significant. Thus, in agreement with both the [^{3}H]flunitrazepam displacement and electrophysiological data, there was no behavioural discrimination between the effects of flurazepam in the two genotypes, indicating that there is

Table 3
Actions of 1 μM zolpidem on mIPSC properties in stellate/basket cells of γ2I77/I77 and γ2F77/F77 mice. Data are presented as mean ± standard deviation. Percent change in each parameter was calculated for each cell and then averaged. Only significant differences within, not between, genotypes are highlighted in italics ($P < 0.05$, Student's paired *t*-test)

mIPSC parameter	Experimental condition	Mouse genotype			
		γ2177/177 ($n = 5$)		γ2F77/F77 ($n = 5$)	
		Absolute data	Percent change	Absolute data	Percent change
Peak amplitude (pA)	Control	−63.0 ± 15.7	2.9 ± 14.6	−64.0 ± 13.4	0.8 ± 7.2
	+1 μM Zolp	−63.2 ± 11.0		−64.1 ± 11.2	
Weighted decay (ms)	Control	3.2 ± 0.7	8.6 ± 3.9	3.5 ± 0.2	84.0 ± 12.4
	+1 μM Zolp	*3.4±0.7*		*6.5±0.7*	
10–90% rise time (μs)	Control	286.0 ± 26.0	2.2 ± 6.8	308.0 ± 35.6	10.5 ± 6.8
	+1 μM Zolp	292.0 ± 28.6		*342.0±61.4*	
Charge transfer (fC)	Control	−231.4 ± 72.0	10.5 ± 13.3	−261.8 ± 50.0	75.0 ± 19.4
	+1 μM Zolp	−251.1 ± 69.5		*−456.5±93.2*	
Frequency (Hz)	Control	1.3 ± 0.5	16.7 ± 44.7	2.5 ± 2.6	26.3 ± 61.9
	+1 μM Zolp	1.4 ± 0.3		2.9 ± 2.6	
Total current (pA)	Control	−0.29 ± 0.09	28.9 ± 52.2	−0.70 ± 0.78	123.5 ± 117.5
	+1 μM Zolp	−0.36 ± 0.12		−1.44 ± 1.48	

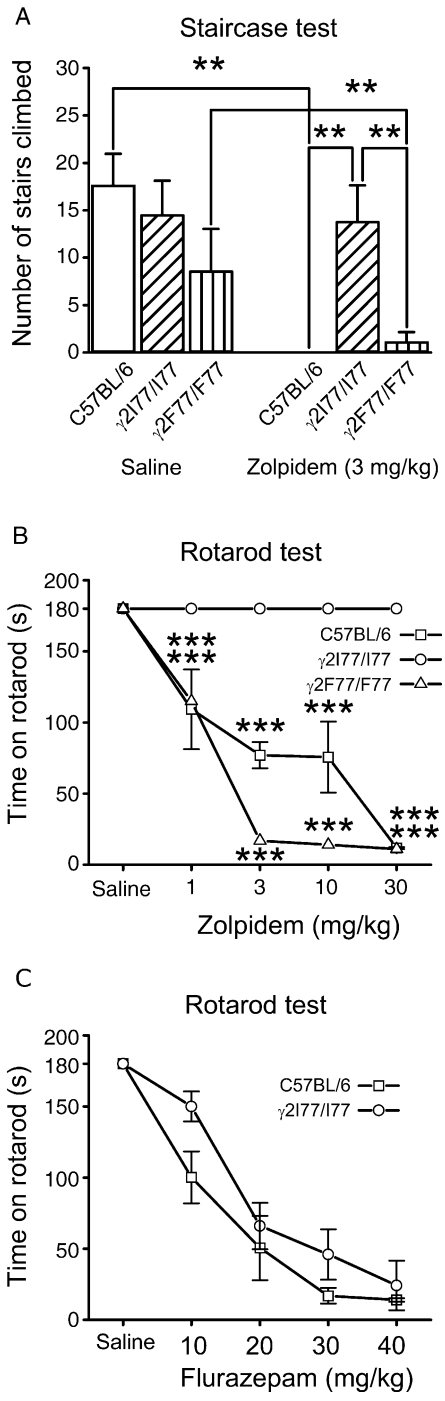

Fig. 9. Exploratory and motor behaviour are zolpidem insensitive in γ2I77/I77 mice. (A) Effects of zolpidem injection (3 mg/kg i.p.) on exploratory behaviour as tested with the staircase test 30 min after administration. Note that exploratory behaviour of γ2I77/I77 mice was not affected by zolpidem, but was significantly reduced in both C57BL/6 and γ2F77/F77 mice, compared to saline injection. (B, C) Effect of zolpidem (B, cumulative dose 1–30 mg/kg i.p.) and flurazepam (C, cumulative dose 10–40 mg/kg i.p.) injection on motor performance as tested with the rotarod 15 min after administration. Cumulative doses of zolpidem increasingly reduced the ability of C57BL/6 and γ2F77/F77 mice to remain on the rotarod without affecting γ2I77/I77 mice. Cumulative doses of flurazepam reduced the ability of both C57BL/6 and γ2I77/I77 mice to remain on the rotarod equally. ** indicates $P < 0.01$ and *** $P < 0.001$, ANOVA with post hoc Neumann–Keuls.

no effect of the point mutation on the binding of flurazepam to the BZ binding site.

4. Discussion

Apparently, "neutral" gene polymorphisms may have a strong influence on nervous system function, therefore it is necessary to control for differences between mouse strains on many parameters. Often, the cohort of genes behind these differences remains elusive. Strong mouse strain differences in BZ sensitivity exist, but the molecular details are not known (e.g. Belzung et al., 2000; Griebel et al., 2000). As part of a larger strategy to develop sets of transgenic mice for investigating nervous system function we engineered a likely "neutral polymorphism" (F77I) into the γ2 subunit gene of the mouse $GABA_A$ receptor and probed for the synaptic and behavioural consequences.

The main findings of this study are: (i) behavioural as well as synaptic actions of zolpidem on Purkinje cells are completely abolished in mice with the γ2F77I point mutation; (ii) a small residual effect of zolpidem on mIPSCs remains in stellate/basket cells of γ2I77/I77 mice; (iii) mIPSCs of Purkinje cells decay somewhat faster in γ2I77/I77 mice compared to C57BL/6 and γ2F77/F77 mice; (iv) quantal GABA release does not appear to saturate postsynaptic $GABA_A$ receptors under control conditions in Purkinje cells; (v) the γ2F77I mutation has no major effect on the expression of $GABA_A$ receptor subunits and total amount of $GABA_A$ receptors in the cerebellum.

4.1. Actions of zolpidem are largely abolished in γ2F77I mice

The potentiation of mIPSCs in Purkinje cells of C57BL/6 and γ2F77/F77 mice by zolpidem was eliminated in γ2I77/I77 mice. Surprisingly, in stellate/basket cells of γ2I77/I77 mice, zolpidem caused a 9% increase in mIPSC weighted decay. Although the increase was 84% in the γ2F77/F77 mice, the small residual increase in γ2I77/I77 mice is unexpected because rodent stellate/basket cells mainly express mRNA for the α1, β2 and γ2 receptor subunits, as do Purkinje cells (Wisden et al., 1992, 1996), in addition to some α3 subunit, at least in the rat (Wisden et al., 1992). It is possible that whereas the F77 residue is required for zolpidem binding in the BZ pocket formed by α1 and γ2 subunits, it is less important for zolpidem binding in the BZ pocket formed by α3 and γ2 subunits. Another possible explanation is that this residual BZ site agonist effect of zolpidem is mediated by receptors containing the γ1 subunit, which are sensitive to zolpidem (Puia et al., 1991; Wingrove et al., 1997). There is, however, no evidence for the expression of γ1

subunit in the cerebellar molecular layer, except in Bergman glial cells (Wisden et al., 1992; Pirker et al., 2000). There is also a weak γ3 subunit-like immunoreactivity expression in the rat, but little or no mRNA has been detected (Pirker et al., 2000). It is unlikely that residual effects are mediated by γ3 subunit containing receptors as they are zolpidem-insensitive (Korpi et al., 2002).

In behavioural experiments, zolpidem sedated C57BL/6 and γ2F77/F77 mice dose dependently in both the exploratory and motor performance tests, whereas γ2I77/I77 mice were unaffected, demonstrating that the effects of zolpidem in vivo are abolished. In contrast to both Purkinje and stellate/basket cells, many cell types express many receptor subunits (e.g. Wisden et al., 1992; Pirker et al., 2000), and therefore potentially many different receptor subtypes. Residual, non-γ2 subunit containing receptor mediated synaptic effects of zolpidem therefore may persist throughout the CNS. However, the complete lack of zolpidem sensitivity of γ2I77/I77 mice in these initial behavioural experiments indicates that such residual effects are too small to affect the behaviour of the animals in these tests to a detectable extent.

The expressions and distributions of the major $GABA_A$ receptor subunits found in the cerebellum were similar between mice with the γ2F77I point mutation and wild-type littermates. The expression of the γ2 subunit decreased by about 15% in the γ2I77/I77 mice, as tested by western blots, but this change was not detectable by immunohistochemistry or [^{3}H]muscimol binding to membranes. The tissue used for western blotting and binding included the deep cerebellar nuclei, but there was no immunohistochemically detectable change in either the cerebellar cortex or the deep cerebellar nuclei. It is likely that such a small change is below detectability in histological sections. The γ2F77I substitution may have slightly altered the processing or stability of the subunit before it is assembled into fully functional receptors, because the residue is predicted to be at the α and γ2 subunit interface.

4.2. Actions of BZ site agonists on Purkinje and stellate/basket cell mIPSCs

Application of zolpidem to Purkinje cells of both C57BL/6 and γ2F77/F77 mice potentiated mIPSCs by increasing both the decay and peak amplitude of these synaptic events, which together led to an increase in $GABA_A$ receptor mediated charge transfer through the membrane. We observed a large increase in the peak amplitude of mIPSCs following zolpidem application in both C57BL/6 and γ2F77/F77 mice. This increase for both genotypes indicates that $GABA_A$ receptors are not saturated by quantal GABA release under control conditions at our recording temperature (33–34 °C). Zolpidem has been used to determine receptor occupancy in several cell types (De Koninck and Mody, 1994; Perrais and Ropert, 1999; Hájos et al., 2000). In these studies, it has been observed that receptors are not saturated at room temperature (i.e. zolpidem increases peak amplitude), but are saturated at more physiological temperatures (i.e. zolpidem does not increase peak amplitude). However, it has been suggested that zolpidem does not behave as a full BZ site agonist at physiological temperatures (Perrais and Ropert, 1999), and that receptors are in fact not saturated at these temperatures. The increase in amplitude that we observed at 33–34 °C would appear to contradict this conclusion, but several differences in recording conditions should be taken into account. First, our study examined the effects of zolpidem on mIPSCs in Purkinje cells. Previous studies on Purkinje cells reported zolpidem effects on currents induced by exogenously applied GABA under steady state conditions, but mIPSCs were not tested (e.g. Sur et al., 2001). Second, we observed large variability in the increase in peak amplitude by zolpidem between individual cells (e.g. −14% to 70% for C57BL/6 mice), so any significant increase may not have been revealed if we recorded from only a few cells. Third, we have recorded cells in the mouse, whereas most previous studies reported results in the rat. Intriguingly, in stellate/basket cells of γ2F77/F77 mice, whereas zolpidem potentiated mIPSCs through a large increase in decay, as shown previously (Vicini et al., 2001), there was no significant increase in the peak amplitude. Therefore, it appears that at 33–34 °C $GABA_A$ receptors of stellate/basket cells are saturated by quantal GABA release. However, the caveats regarding the experimental conditions of Purkinje cell recordings also apply for stellate/basket cell recordings.

Flurazepam had similar effects on mIPSCs recorded in Purkinje cells from all three mouse genotypes. The potentiating effects of flurazepam in C57BL/6 and γ2F77/F77 mice were smaller than those described for zolpidem. This is probably due to zolpidem being a more efficacious agonist at α1 subunit containing receptors than flurazepam. In all three genotypes, flurazepam caused a significant increase in the peak amplitude of the mIPSCs, further suggesting that $GABA_A$ receptors expressed by Purkinje cells are not saturated by quantal GABA release under our control conditions.

Our results with flurazepam are similar to previously reported results in cerebellar stellate cells (Nusser et al., 1997). These authors observed a large increase in both peak amplitude and weighted decay at room temperature. The increase in peak amplitude was only observed for large mIPSCs in these cells. Furthermore, Nusser et al. (1997) reported that mIPSC amplitude, the number of $GABA_A$ receptors in a synapse and the size of a synapse are correlated. They concluded that small

mIPSCs are generated by activation of few $GABA_A$ receptors in small synapses, which are therefore saturated under control conditions. In contrast, large mIPSCs were suggested to be generated by activation of many $GABA_A$ receptors in large synapses, where not all receptors are activated by quantal GABA release, and thus their occupancy can be enhanced by flurazepam. Displaying our data in cumulative probability plots also showed that in most Purkinje cells the peak amplitude of only the large mIPSCs was increased by both zolpidem and flurazepam, whereas mIPSCs smaller than −30 to −40 pA were not affected.

We observed a 13% decrease in the weighted decay and consequently in charge transfer of mIPSCs in Purkinje cells of γ2I77/I77 mice prior to any drug application that could not be explained by genetic background, age, or recording temperature. One possible explanation is that the γ2F77I point mutation reduces the binding of an endogenous BZ site agonist that functionally contributes to the kinetics of mIPSCs. However, such an effect was not observed on stellate/basket cells, and the testing of more cell types as well as pharmacological experiments are needed to investigate this possibility.

In previous studies, homozygous γ2 knockout mice were shown to die early probably due to impaired postsynaptic receptor clustering and loss of $GABA_A$ receptor function (Günther et al., 1995; Essrich et al., 1998). However, heterozygous γ2 knockout mice were reported as a model of anxiety (Crestani et al., 1999). In addition, mice with a point mutation in the $GABA_A$ α1 subunit have been generated and used to investigate the contribution of α1 subunit-containing receptors to the pharmacological actions of BZ site ligands (Rudolph et al., 1999; McKernan et al., 2000). In mice with the α1H101R point mutation, the binding of zolpidem and diazepam to α1 subunit containing $GABA_A$ receptors was abolished without altering receptor number or composition (Rudolph et al., 1999; McKernan et al., 2000), and GABAergic postsynaptic currents were less affected by zolpidem in some cell types than in others (Bacci et al., 2003). Mice with the α1H101R point mutation showed reduced sedative, amnesic and partly anticonvulsant effects of diazepam, with little effect on its anxiolytic, myorelaxant, motor performance impairing and ethanol potentiating actions (Rudolph et al., 1999; McKernan et al., 2000). The sedative–hypnotic actions of zolpidem are abolished in the α1H101R mice and are therefore mediated by α1 subunit-containing receptors (Crestani et al., 2000). The α1H101R and the γ2I77/I77 point mutant mice, both with reduced zolpidem sensitivity, are expected to respond differently to zolpidem challenge in some behavioural tasks because the γ2F77I point mutation not only impairs interaction with α1 subunit-containing receptors, but also with all other γ2 subunit-containing receptors. Here, we have shown that zolpidem impairment of exploratory activity and motor performance, which have a known cerebellar contribution, is abolished in the γ2F77I mice. Due to the apparent neutrality of the γ2F77I point mutation, γ2I77/I77 mice may be useful in discerning physiological roles of γ2 subunit-containing receptors. Furthermore, whereas the α1 point mutant mice may be useful for investigating the roles of specific α subunit-containing $GABA_A$ receptor subtypes in the brain, the γ2F77I mice may be used to further elucidate the actions of the popular clinical hypnotic zolpidem, and the subtypes of $GABA_A$ receptors involved, given its α subunit selectivity.

In summary, the γ2F77I point mutation resulted in a mouse insensitive to zolpidem but sensitive to other BZ agonists. The γ2I77/I77 mouse may help to dissect the differential pharmacological and physiological contributions of zolpidem-sensitive $GABA_A$ receptors in the brain by restoring zolpidem sensitivity to selected brain regions and neuronal populations.

Acknowledgements

We wish to thank Mrs. E. Norman (MRC Anatomical Neuropharmacology Unit, Oxford, UK) for her excellent technical assistance, Dr. Laszlo Marton (MRC Anatomical Neuropharmacology Unit, Oxford, UK) for his help with some of the statistical tests, and Dr. A.F. Stewart (MPI, Dresden, Germany) for the gift of the pCAGGS-FLPe vector. Drs. Mark Farrant, Beverley Clark (UCL, London, UK) and Zoltan Nusser (Inst. Exp. Med., Budapest, Hungary) provided helpful advice for recording stellate/basket cells. We thank Dr. Zoltan Nusser for helpful comments on a previous version of this manuscript. C.H. held a European H. Blaschko Research Scholarship. This work was also supported by the Academy of Finland to E.R.K., by project P14385-GEN of the Austrian Science Fund to W.S., and by the VolkswagenStiftung, grant I/78 554, to W.W.

References

Bacci, A., Rudolph, U., Huguenard, J.R., Prince, D.A., 2003. Major differences in inhibitory synaptic transmission onto two neocortical interneuron subclasses. Journal of Neuroscience 23, 9664–9674.

Belzung, C., Le Guisquet, A.M., Crestani, F., 2000. Flumazenil induces benzodiazepine partial agonist-like effects in BALB/c but not C57BL/6 mice. Psychopharmacology (Berlin) 148, 24–32.

Buhr, A., Baur, R., Sigel, E., 1997. Subtle changes in residue 77 of the γ subunit of α1β2γ2 $GABA_A$ receptors drastically alter the affinity for ligands of the benzodiazepine binding site. Journal of Biological Chemistry 272, 11799–11804.

Cope, D.W., Wulff, P., Oberto, A., Jones, A., Hoeger, H., Capogna, M., Ferraguti, F., Sieghart, W., Korpi, E.R., Wisden, W., Somogyi, P., 2003. Abolition of zolpidem potentiation of $GABA_A$ receptor mediated mIPSCs in neurones of γ2 subunit point mutant mice. Society for Neuroscience Abstracts 47, 13.

Crestani, F., Lorez, M., Baer, K., Essrich, C., Benke, D., Laurent, J.P., Belzung, C., Fritschy, J.-M., Lüscher, B., Mohler, H., 1999. Decreased $GABA_A$-receptor clustering results in enhanced anxiety and a bias for threat cues. Nature Neuroscience 2, 823–839.

Crestani, F., Martin, J.R., Möhler, H., Rudolph, U., 2000. Mechanism of action of the hypnotic zolpidem in vivo. British Journal of Pharmacology 131, 1251–1254.

De Koninck, Y., Mody, I., 1994. Noise analysis of miniature IPSCs in adult rat brain slices: properties and modulation of synaptic $GABA_A$ receptor channels. Journal of Neurophysiology 71, 1318–1335.

Ernst, M., Brauchart, D., Boresch, S., Sieghart, W., 2003. Comparative modeling of $GABA_A$ receptors: limits, insights, future developments. Neuroscience 119, 933–943.

Essrich, C., Lorez, M., Benson, J.A., Fritschy, J.-M., Lüscher, B., 1998. Postsynaptic clustering of major $GABA_A$ receptor subtypes requires the γ2 subunit and gephyrin. Nature Neuroscience 1, 563–571.

Griebel, G., Belzung, C., Perrault, G., Sanger, D.J., 2000. Differences in anxiety-related behaviours and in sensitivity to diazepam in inbred and outbred strains of mice. Psychopharmacology (Berlin) 148, 164–170.

Günther, U., Benson, J., Benke, D., Fritschy, J.-M., Reyes, G., Knoflach, F., Crestani, F., Aguzzi, A., Arigoni, M., Lang, Y., Bluethmann, H., Mohler, H., Lüscher, B., 1995. Benzodiazepine-insensitive mice generated by targeted disruption of the γ2 subunit gene of γ-aminobutyric acid type A receptors. Proceedings of the National Academy of Sciences USA 92, 7749–7753.

Hájos, N., Nusser, Z., Rancz, E.A., Freund, T.F., Mody, I., 2000. Cell type- and synapse-specific variability in synaptic $GABA_A$ receptor occupancy. European Journal of Neuroscience 12, 810–818.

Jechlinger, M., Pelz, R., Tretter, V., Klausberger, T., Sieghart, W., 1998. Subunit composition and quantitative importance of hetero-oligomeric receptors: $GABA_A$ receptors containing α6 subunits. Journal of Neuroscience 18, 2449–2457.

Jensen, K., Mody, I., 2001. GHB depresses fast excitatory and inhibitory synaptic transmission via $GABA_B$ receptors in mouse neocortical neurons. Cerebral Cortex 11, 424–429.

Jones, A., Korpi, E.R., McKernan, R.M., Pelz, R., Nusser, Z., Mäkela, R., Mellor, J.R., Pollard, S., Bahn, S., Stephenson, F.A., Randall, A.R., Sieghart, W., Somogyi, P., Smith, A.J.H., Wisden, W., 1997. Ligand-gated ion channel subunit partnerships: $GABA_A$ receptor α6 subunit gene inactivation inhibits δ subunit expression. Journal of Neuroscience 17, 1350–1362.

Korpi, E.R., Gründer, G., Lüddens, H., 2002. Drug interactions at $GABA_A$ receptors. Progress in Neurobiology 67, 113–159.

Kralic, J.E., Korpi, E.R., O'Buckley, T.K., Homanics, G.E., Morrow, A.L., 2002. Molecular and pharmacological characterization of $GABA_A$ receptor α1 subunit knockout mice. Journal of Pharmacology and Experimental Therapeutics 302, 1037–1045.

Llano, I., Marty, A., 1995. Presynaptic metabotropic glutamatergic regulation of inhibitory synapses in rat cerebellar slices. Journal of Physiology 486, 163–176.

McKernan, R.M., Rosahl, T.W., Reynolds, D.S., Sur, C., Wafford, K.A., Atack, J.R., Farrar, S., Myers, J., Cook, G., Ferris, P., Garrett, L., Bristow, L., Marshall, G., Macaulay, A., Brown, N., Howell, O., Moore, K.W., Carling, R.W., Street, L.J., Castro, J.L., Ragan, C.I., Dawson, G.R., Whiting, P.J., 2000. Sedative but not anxiolytic properties of benzodiazepines are mediated by the $GABA_A$ receptor α1 subtype. Nature Neuroscience 3, 587–592.

Nusser, Z., Cull-Candy, S., Farrant, M., 1997. Differences in synaptic $GABA_A$ receptor number underlie variation in GABA mini amplitude. Neuron 19, 697–709.

Perrais, D., Ropert, N., 1999. Effect of zolpidem on miniature IPSCs and occupancy of postsynaptic $GABA_A$ receptors in central synapses. Journal of Neuroscience 19, 578–588.

Pirker, S., Schwarzer, C., Wieselthaler, A., Sieghart, W., Sperk, G., 2000. $GABA_A$ receptors: immunocytochemical distributions of 13 subunits in the adult rat brain. Neuroscience 101, 815–850.

Pöltl, A., Hauer, B., Fuchs, K., Tretter, V., Sieghart, W., 2003. Subunit composition and quantitative importance of $GABA_A$ receptor subtypes in the cerebellum of mouse and rat. Journal of Neurochemistry 87, 1444–1455.

Puia, G., Vicini, S., Seeburg, P.H., Costa, E., 1991. Influence of recombinant γ-aminobutyric acid-$_A$ receptor subunit composition on the action of allosteric modulators of γ-aminobutyric acid-gated Cl^- currents. Molecular Pharmacology 39, 691–696.

Rogers, D.C., Jones, D.N., Nelson, P.R., Jones, C.M., Quilter, C.A., Robinson, T.L., Hagan, J.J., 1999. Use of SHIRPA and discriminant analysis to characterise marked differences in the behavioural phenotype of six inbred mouse strains. Behavioural Brain Research 105, 207–217.

Rudolph, U., Crestani, F., Benke, D., Brünig, I., Benson, J.A., Fritschy, J.-M., Martin, J.R., Bluethmann, H., Möhler, H., 1999. Benzodiazepine actions mediated by specific γ-aminobutyric $acid_A$ receptor subtypes. Nature 401, 796–800.

Schaft, J., Ashery-Padan, R., van der Hoeven, F., Gruss, P., Stewart, A.F., 2001. Efficient FLP recombination in mouse ES cells and oocytes. Genesis 31, 6–10.

Sieghart, W., 1995. Structure and pharmacology of γ-aminobutyric $acid_A$ receptor subtypes. Pharmacological Reviews 47, 181–234.

Sieghart, W., Sperk, G., 2002. Subunit composition, distribution and function of $GABA_A$ receptor subtypes. Current Topics in Medicinal Chemistry 2, 795–816.

Sigel, E., 2002. Mapping of the benzodiazepine recognition site on $GABA_A$ receptors. Current Topics in Medicinal Chemistry 2, 833–839.

Somogyi, P., Takagi, H., Richards, J.G., Mohler, H., 1989. Subcellular localization of benzodiazepine/$GABA_A$ receptors in the cerebellum of rat, cat and monkey using monoclonal antibodies. Journal of Neuroscience 9, 2197–2209.

Southan, A.P., Robertson, B., 1998. Patch-clamp recordings from cerebellar basket cell bodies and their presynaptic terminals reveal an asymmetric distribution of voltage-gated potassium channels. Journal of Neuroscience 18, 948–955.

Sur, C., Wafford, K.A., Reynolds, D.S., Hadingham, K.L., Bromidge, F., Macaulay, A., Collinson, N., O'Meara, G., Howell, O., Newman, R., Myers, J., Atack, J.R., Dawson, G.R., McKernan, R.M., Whiting, P.J., Rosahl, T.W., 2001. Loss of the major $GABA_A$ receptor subtype in the brain is not lethal in mice. Journal of Neuroscience 21, 3409–3418.

Thomson, A.M., Bannister, A.P., Hughes, D.I., Pawelzik, H., 2000. Differential sensitivity to zolpidem of IPSPs activated by morphologically identified CA1 interneurons in slices of rat hippocampus. European Journal of Neuroscience 12, 425–436.

Vicini, S., Ferguson, C., Prybylowski, K., Kralic, J., Morrow, A.L., Homanics, G.E., 2001. $GABA_A$ receptor α1 subunit deletion prevents developmental changes in inhibitory synaptic currents in cerebellar neurons. Journal of Neuroscience 21, 3009–3016.

Wessel, D., Flügge, U.I., 1984. A method for quantitative recovery of protein in dilute solution in the presence of detergents and lipids. Analytical Biochemistry 138, 141–143.

Wingrove, P.B., Thompson, S.A., Wafford, K.A., Whiting, P.J., 1997. Key amino acids in the γ subunit of the γ-aminobutyric $acid_A$ receptor that determine ligand binding and modulation at the benzodiazepine site. Molecular Pharmacology 52, 874–881.

Wisden, W., Laurie, D.J., Monyer, H., Seeburg, P.H., 1992. The distribution of 13 $GABA_A$ receptor subunit mRNAs in the rat brain. I. Telencephalon, diencephalon, mesencephalon. Journal of Neuroscience 12, 1040–1062.

Wisden, W., Korpi, E.R., Bahn, S., 1996. The cerebellum: a model system for studying $GABA_A$ receptor diversity. Neuropharmacology 35, 1139–1160.

Zhang, C.-L., Messing, A., Chiu, S.Y., 1999. Specific alteration of spontaneous GABAergic inhibition in cerebellar Purkinje cells in mice lacking the potassium channel Kv1.1. Journal of Neuroscience 19, 2852–2864.